Application of Microwave Superheating for the Synthesis of TiO₂ Rods

Vilas G. Pol,*,† Yaakov Langzam,‡ and Arie Zaban†

Department of Chemistry, Nano-energy Research Center, Institute of Nanotechnology and Advanced Materials, and Faculty of Life Sciences, Bar-Ilan University, Ramat-Gan 52900, Israel

A simple microwave irradiation method for the large-scale synthesis of submicrometer-sized TiO₂ rods at normal atmospheric pressure and the boiling temperature of the solvent is demonstrated. It is emphasized that only 1−3 min of microwave irradiation is adequate to react tetra-isopropyl orthotitanate with ethylene glycol to produce rods of titanium glycolate [TG] with diameters of ∼0.4 μm and lengths up to 5 μm. The as-formed TG rods, followed by calcination under air for 2 h, fabricated anatase (500 °C) and rutile (900 °C) titania without changing their rod-shaped morphology. The crystallinity, structure, morphology, and thermal analysis are carried out by several techniques. A mechanism based on microwave superheating phenomena is presented with the support of previous reports and several control experiments.

Introduction

One-dimensional nanostructured materials have attracted considerable attention recently due to their unique physical properties and their potential applications in nanoelectronics and optoelectronics devices.[1] Titanium dioxide is an n-type semiconductor and a typical photocatalyst, attracting much attention from both fundamental and practical viewpoints. It has been used in many industrial areas, e.g., in water purification, gas sensors, pigments, and cosmetics.[2] TiO₂ has also been demonstrated as a promising electron-transport material for dye-sensitized oxide semiconductor solar cells.[3] Recently, the use of one-dimensional (1D) nanostructures instead of nanocrystalline films in photoelectrochemical cells has been considered.[3,4] In addition, a more than 2-fold increase in maximum photoconversion efficiency for water splitting has been observed by replacing TiO₂ nanocrystalline films with TiO₂ nanowires.[4]

The growth of 1D TiO₂ nanostructures, including nanowires and nanotubes, has been demonstrated using sol−gel, electrodeposition, and hydrothermal methods with or without anodic aluminum oxide (AAO).[5] Well-aligned rutile and anatase TiO₂ nanorods, as well as anatase TiO₂ nanowalls, have been synthesized using a template- and catalyst-free metal/organic chemical vapor deposition method.[6] Recently, TiO₂ nanorods were synthesized by heating a sol−gel template process; the rods are composed of ∼10 nm TiO₂ nanoparticles.[7]

Rutile-type TiO₂ rods were grown on the glass substrates through heterogeneous nucleation in TiCl₃ aqueous solutions at low temperatures (80 °C) under hydrothermal conditions.[8] The simultaneous phase- and size-controlled synthesis of TiO₂ nanorods was achieved via the non-hydrolytic sol−gel reaction of continuously delivered two titanium precursors using two separate syringe pumps.[9] Rutile TiO₂ nanowhiskers have been synthesized by annealing[10] a precursor powder in which NaCl and Ti(OH)ₓ particles were homogeneously mixed. Hsiech et al. used a light-emitting amphiphilic molecule [PEO17-OPV3] as a structure-directing agent to fabricate the nanohollow titania rods[11] through self-assembly. Cozzoli et al. demonstrated the controlled growth of high aspect ratio anatase TiO₂ nanorods by hydrolysis[12] of titanium tetra-isopropoxide in oleic acid surfactant at 80 °C. Surfactant-assisted elimination of a high-energy facet as a means of controlling the shapes[13] of TiO₂ nanocrystals is studied by Jun et al. Hydrothermal synthesis of single-crystalline anatase TiO₂ nanorods are also prepared using nanotubes as the precursor.[14] The growth of TiO₂ pillars[15] by chemisorbed nanotitania followed by annealing is also accounted recently.

There are several reports in the literature on the fabrication of titania nanotubes by the hydrothermal treatment[16] of titania particles with a NaOH solution at various temperatures. However, there are discrepancies in the purity and in the mechanism for the formation of the TiO₂ nanotubes, as well as in the conclusions. In this article, we demonstrate the simplest, most efficient approach to synthesize submicrometer-sized titanium glycolate rods within 3 min of microwave irradiation. Not only time but also the energy required to carry out such reactions can be saved with the microwave route of syntheses. Since titania is not a layered compound, this is one of the ways to incorporate nanosize particles together to build a 1D morphology of TiO₂. The main advantage is that after the sintering process the 1D morphology continues to persist with the pure anatase and rutile phases of titania. This is not possible with the titania-based nanotubes[16]

* Corresponding author. E-mail: vilaspol@gmail.com.
† Department of Chemistry.
‡ Faculty of Life Sciences.

(1) Diebold, U. *Surf. Sci. Rep.* **2003**, *48*, 53.
(2) Gratzel, M. *Nature* **2001**, *414*, 338.
(3) Huynh, W. U.; Dittmer, J. J.; Alivisatos, A. P. *Science* **2002**, *295*, 2425.
(4) Khan, S. U. M.; Sultana, T. *Sol. Energy Mater. Sol. Cells* **2003**, *76*, 211.
(5) (a) Lakshmi, B. B.; Dorhout, P. K.; Martin, C. R. *Chem. Mater.* **1997**, *9*, 857. (b) Kasuga, T.; Hiramatsu, M.; Hoson, A.; Sekino, T.; Niihara, K. *Langmuir* **1998**, *14*, 3160. (c) Zhang, X. Y.; Zhang, L. D.; Chen, W.; Meng, G. W.; Zheng, M. J.; Zhao, L. X. *Chem. Mater.* **2001**, *13*, 2511. (d) Kasuga, T.; Hiramatsu, M.; Hoson, A.; Sekino, T.; Niihara, K. *Adv. Mater.* **1999**, *11*, 1307.
(6) Wu, J. J.; Yu, C. C. *J. Phys. Chem. B* **2004**, *108*, 3379.
(7) Miao, L.; Tanemura, S.; Toh, S.; Kaneko, K.; Tanemura, M. *J. Cryst. Growth* **2004**, *264*, 246.
(8) Kakiuchi, K.; Hosono, E.; Imai, H.; Kimura, T.; Fujihara, S. *J. Cryst. Growth* **2006**, *293*, 541.

(9) Koo, B.; Park, J.; Kim, Y.; Choi, S. H.; Sung, Y. E.; Hyeon, T. *J. Phys. Chem. B* **2006**, *110*, 24318.
(10) Li, G. L.; Wang, G. H.; Hong, J. M. *J. Mater. Res.* **1999**, *14*, 3346.
(11) Hsiech, C. C.; Lin, K. F.; Chien, A. T. *Macromolecules* **2006**, *39*, 3043.
(12) Cozzoli, P. D.; Kornowski, A.; Weller, H. *J. Am. Chem. Soc.* **2003**, *125*, 14539.
(13) Jun, Y. W.; Casula, M. F.; Sim, J. H.; Kim, S. Y.; Cheon, J.; Alivisatos, A. P. *J. Am. Chem. Soc.* **2003**, *125*, 15981.
(14) Nian, J. N.; Teng, H. S. *J. Phys. Chem. B* **2006**, *110*, 4193.
(15) Pol, V. G.; Zaban, A. *J. Phys. Chem. C* **2007**, *111*, 13313.
(16) (a) Lakshmi, B. B.; Dorhout, P. K.; Martin, C. R. *Chem. Mater.* **1997**, *9*, 857. (b) Kasuga, T.; Hiramatsu, M.; Hoson, A.; Sekino, T.; Niihara, K. *Langmuir* **1998**, *14*, 3160. (c) Zhang, X. Y.; Zhang, L. D.; Chen, W.; Meng, G. W.; Zheng, M. J.; Zhao, L. X. *Chem. Mater.* **2001**, *13*, 2511. (d) Kasuga, T.; Hiramatsu, M.; Hoson, A.; Sekino, T.; Niihara, K. *Adv. Mater.* **1999**, *11*, 1307.

Table 1. Reagents, Reaction Time, and Product Obtained after Calcination at 500 °C

sample no.	reagents[a]	reaction time (min)	product annealed at 500 °C	morphology (SEM)[b]
1	EG + tetra-isopropyl orthotitanate (1 mL)	1	anatase TiO$_2$	rods + nanoparticles: rod diameter = 350 nm rod length = 5 μm nanoparticles = 12 nm
2	EG + tetra-isopropyl orthotitanate (1 mL)	3	anatase TiO$_2$	rods: diameter = 400 nm length = 5.5 μm
3	EG + tetra-isopropyl orthotitanate (2 mL)	3	anatase TiO$_2$	rods: diameter = 800 nm length = 20 μm
4	EG + tetra-isopropyl orthotitanate (0.2 mL)	3	anatase TiO$_2$	rods: diameter = 400 nm length = 5 μm
5	EG + titanium (IV) 2-ethylhexoxide	3	anatase TiO$_2$	rods: diameter = 5−10 μm length = 20−100 μm
6	TEG + tetra-isopropyl orthotitnate	3	anatase TiO$_2$	particles diameter = 200 nm
7	EG + isopropanol + tetra-isopropyl orthotitanate (1 mL)	3	anatase TiO$_2$	particles diameter = 150 nm
8	EG + water + tetra-isopropyl orthotitanate (1 mL)	3	anatase TiO$_2$	particles diameter = 100 nm

[a] EG = ethylene glycol, TEG = triethylene glycol. [b] The achieved morphologies are illustrated.

grown in alkali medium since the nanotubes collapse back to nanoparticles after the sintering process. On the other hand, we could achieve pure rods composed of anatase or rutile titania nanocrystals with a nanoporous geometry in the bulk quantity using a competent microwave method.

Since the early 1940s, microwave heating has been known and successfully used in the food industry. Microwave irradiation as a reflux heating method[17−20] has found a number of applications in chemistry since 1986. Many thriving examples of the applications of microwave heating in organic chemistry have been reported,[21] although its expansion to inorganic chemistry has been much slower. The effect of heating is created by the interaction of the dipole moment of the molecules with the high-frequency electromagnetic radiation (2.45 GHz). However, there are many microwave phenomena which are poorly understood, such as nonthermal effects and the superheating effect.[22] The microwave-assisted synthesis of rod-shaped metals [e.g., Ag,[23] Au,[24] Se,[25] Te[26]], metal oxides [e.g., copper oxide,[27] Ga$_2$O$_3$,[28] ZnO[29]], and sulfides [e.g., copper sulfide[30]] is already known. We report herein on the shortest synthesis time for producing rod-shaped titanium glycolates that transform into pure TiO$_2$

after 2-h calcinations, 500 °C for pure anatase and 900 °C for pure rutile. The calcinated materials maintain the rodlike morphology of the titanium glycolates.

Experimental Section

In a typical synthesis, 1 mL of tetra-isopropyl orthotitanate [Merck comp] was added to a round-bottomed flask containing 50 mL of ethylene glycol. All the operations were performed inside a glove box purged with nitrogen gas. The solution was placed in the glove box in a 100-mL round-bottomed flask. The solution was then removed from the glove box and irradiated with 100% microwave power (900 W, at 2.45 GHz). The microwave refluxing apparatus was a modified domestic microwave oven that has been described elsewhere.[31] After 1 min of microwave irradiation a white flocculate was observed, indicating the transformation of the titanium alkoxide into a chainlike, titanium glycolate complex. The microwave irradiation was continued for a further 2 min. The slurry was centrifuged at 8000 rpm and washed twice with ethanol and with distilled water and then was dried under vacuum for 12 h.

Characterization

The structure and phase purity of the as-synthesized and calcined samples were examined by XRD analysis using a Bruker AXS D8 Advance Powder X-ray diffractometer (using Cu Kα, wavelength = 1.5418 A° radiation) operating at 40 kV/40 mA. The surface area was measured by N$_2$ adsorption and calculated using a BET equation with a Micrometrics Gemini instrument. To determine the percentage of elemental carbon and hydrogen in the as-synthesized and calcined materials, elemental analysis was carried out on EA 1110 C, H, N, S−O, CE Instruments. The TGA of the as-synthesized TG material was carried out under a stream of nitrogen at a heating rate of 10 °C/min from 30 °C to 950 °C, using a Mettler TGA/STDA 851 instrument. The DSC of the as-synthesized TG sample was carried out on a Mettler Toledo TC 15 model, at a heating rate of 10 °C/min in a crimped

(17) Mingos, D. M. P. *Chem. Ind.* **1994**, 596.
(18) Mingos, D. M. P. *Res. Chem. Intermed.* **1994**, *20*, 85.
(19) Baghurst, D. R.; Mingos, D. M. P. *J. Chem. Soc., Chem. Commun.* **1992**, 674.
(20) Whittaker, A. G.; Mingos, D. M. P. *J. Chem. Soc., Dalton Trans.* **1995**, 2073.
(21) Caddick, S. *Tetrahedron* **1995**, *51*, 10403.
(22) Roy, R. J. *Solid State Chem*. **1994**, *111*, 11.
(23) Liu, F. K.; Chang, Y. C.; Huang, P. W.; Ko, F. H.; Chu, T. C. *Chem. Lett.* **2004**, *33*, 1050.
(24) Tsuji, M.; Hashimoto, M.; Nishizawa, Y.; Tsuji, T. *Mater. Lett.* **2004**, *58*, 2326.
(25) Lu, Q. Y.; Gao, F.; Komarneni, S. *J. Mater. Res.* **2004**, *19*, 1649.
(26) Zhu, Y. J.; Hu, X. L. *Chem. Lett.* **2004**, *6*, 760.
(27) Zhao, Y.; Zhu, J. J.; Hong, J. M.; Bian, N. S.; Chen, H. Y. *Eur. J. Inorg. Chem.* **2004**, *20*, 4072.
(28) Patra, C.; Mastai, Y.; Gedanken, A. *J. Nanopart. Res.* **2004**, *6*, 509.
(29) Hu, X. L.; Zhu, Y. J.; Wing, S. W. *Mater. Chem. Chem. Phys.* **2004**, *88*, 421.
(30) Liao, X. H.; Chen, N. Y.; Xu, S.; Yang, S. B.; Zhu, J. J. *J. Cryst. Growth.* **2003**, *252*, 593.
(31) Palchik, O.; Felner, I.; Kataby, G.; Gedanken, A. *J. Mater. Res.* **2000**, *15*, 2176.
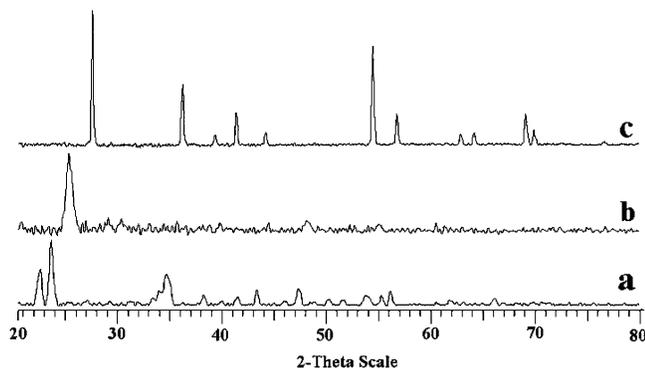
Figure 1. XRD patterns of (a) as-synthesized titanium glycolate, (b) anatase titania [sample 2 annealed at 500 °C], and (c) rutile titania rods [sample 2 annealed at 900 °C].

aluminum crucible in the temperature range of 30−550 °C. The particle morphology (microstructure of the samples) was studied with a TEM (JEOL-JEM 1010SX microscope) working at a 100 kV accelerating voltage and a JEOL-JSM 840 scanning electron microscope. High-resolution TEM (HR-TEM) images were taken using a JEOL-2010 with 200 kV accelerating voltage. Samples for TEM were prepared by dissolving a small quantity of the sample in ethanol and sonicating the solution for 10 min in a vial placed in a sonication bath. One or two drops of the sample suspension (rod solution) were deposited on a copper grid (400 mesh, SPi Suppliers, Westchester, PA) coated with carbon film. When the grid was placed on Whatmann filter paper, it absorbed the droplet and dried the excess solvent in 5−10 min.

Results and Discussion

A typical synthesis of the TiO₂ rods was carried out by the new microwave method, and the results are presented in Table 1. The crystallinity and structure of two as-synthesized and annealed products were measured by XRD and HR-TEM. The as-synthesized materials collected after 1 and 3 min of microwave irradiation (samples 1 and 2, respectively) show almost the same XRD patterns. The XRD pattern of the as-synthesized sample 2, which was collected after 3 min of microwave irradiation (Figure 1a) match perfectly with the reported titanium glycolate.[32] Calcination of the titanium glycolate, sample 2, at 500 °C and 900 °C resulted in anatase and rutile phases, respectively, as seen in the XRD patterns of Figure 1b, (anatase PDF No. 21-1272) and Figure 1c (rutile PDF No. 1-89-4920). Using the Scherrer equation, the crystallite diameters of all three samples were calculated, taking into consideration the full-width at half-maximum (fwhm) of all the peaks. The calculated particle diameters for the titanium glycolate, and the anatase and rutile titania crystals were 17, 14, and 43 nm, respectively.

In the following section, we will show that the as-synthesized titanium glycolate rods are comprised of nanoparticles in a nanoporous geometry which, when sintered, turn into rods consisting of pure anatase or rutile titania nanoparticles. The 1D morphologies of the obtained materials were observed by SEM and TEM. The SEM image (Figure 2a) demonstrates that the rod-shaped morphology of titanium glycolate already appears after 1 min of microwave irradiation. The as-formed titanium glycolate rods had diameters of ∼350 nm and lengths up to 5 μm. The surfaces of these rodlike titanium glycolate complexes are decorated with ∼15 nm particles. When the microwave irradiation lasted a total of 3 min, smooth rods of a titanium glycolate complex with diameters of 400 nm and lengths up to
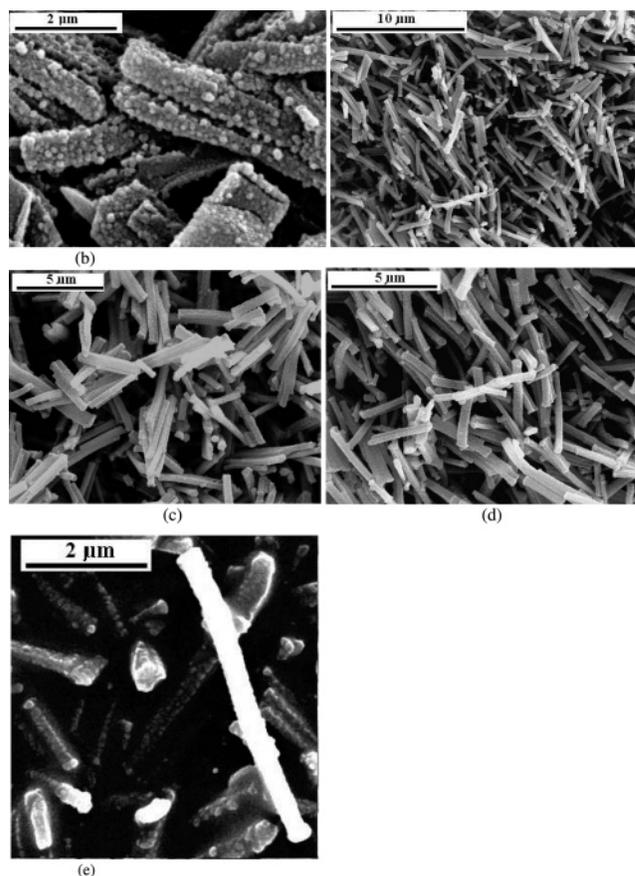

Figure 2. Scanning electron microscopy images of (a) sample 1, (b) sample 2, (c) sample 2 annealed at 500 °C, (d) sample 2 annealed at 900 °C, and (e) the roughness of the individual TiO₂ rods shown at high resolution (sample 2 annealed at 900 °C).

5.5 μm were obtained (Figure 2b), indicating that the rods are formed at the expense of the nanoparticles. SEM images of the calcined titanium glycolate of sample 2 are presented in Figure 2c,d, with Figure 2c following the 500 °C treatment and Figure 2d following the 900 °C process. The images of Figure 2c and d show that the rodlike morphology and the specific dimensions (∼400 nm diameter and 5.5 μm length) are essentially preserved in the calcination process. However, the relatively smooth surfaces of the titanium glycolate complex were significantly roughened, as shown in a typical HR-SEM image (Figure 2e) of an individual TiO₂ rod. The roughness induced by the calcination process could be attributed to the degradation of organic groups and phase transformation. The detailed morphological changes can be seen in the following TEM section. The changes in structure and phase were also identified by the XRD (Figure 1) patterns.

The compositional and structural changes in the titanium glycolate complex associated with thermal annealing were also characterized using C, H, N, S analysis, differential scanning calorimetry (DSC), thermogravimetric analysis (TGA), and Raman spectroscopy. The TGA curve recorded under a flow of nitrogen gas (Figure 3) indicates a three-step weight-loss pattern in the temperature range of 30−100 °C, 150−350 °C, and 350−950 °C. The first weight loss (∼8%) corresponds to physically adsorbed water molecules, and the second one (∼33%) is associated with the removal of ethylene glycol units and the degradation of organic groups contained in the precursor particles.[33] The third slow weight loss of <4% is associated with the degradation of organic groups that are probably located in

(32) Jiang, X.; Wang, Y.; Herricks, T. Xia, Y. *J. Mater. Chem.* **2004**, *14*, 695.

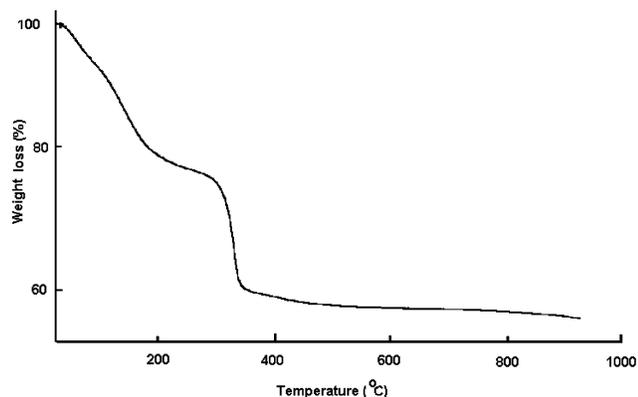(33) Jiang, X.; Herricks, T.; Xia, Y. *Adv. Mater.* **2003**, *15*, 1205.

Figure 3. Thermogravimetric analysis of a titanium glycolate complex carried out under a stream of nitrogen at a heating rate of 10 °C/min.
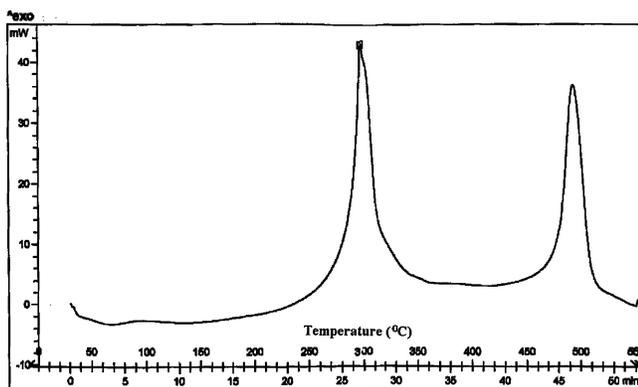

Figure 4. DSC of the as-synthesized TG sample carried out on a Mettler Toledo TC 15 model at a heating rate of 10 °C/ min in a crimped aluminum crucible in the temperature range of 30−550 °C.

Figure 5. Raman spectra of (a) anatase TiO_2 rods and (b) rutile TiO_2 rods.

the inner part of the TiO_2 rods, thus requiring higher temperatures and longer process duration. This understanding is supported by the C, H, N, and S analysis of the annealed materials. The as-prepared titanium glycolate powder contains 22.5% (element) carbon and 5.2% hydrogen. Following annealing at 500 °C, the organic contamination drops to 0.14% carbon and 0.12% hydrogen, while at 900 °C, the process further decreases the percentage of carbon and hydrogen to almost zero.

The DSC pattern of the as-prepared, 1D titanium glycolate complex carried out under air is presented in Figure 4. It shows two broad exothermic peaks. The first peak, ranging from 250 °C and 350 °C, is related to the oxidative combustion of the ethylene glycol units[34] and/or the degradation of the organic groups. The second exotherm, at 470−530 °C, corresponds to the phase transformation from amorphous to anatase titania.

The Raman spectrum of the anatase TiO_2 rods obtained after the 500 °C calcination is presented in Figure 5a. The spectrum consists of six peaks at 144, 200, 398.48 519.54, 643.74, and 801 cm^{-1}, respectively. Following refs 35,36 with respect to both position and intensity, we assign these peaks to the E_g, E_g, B_{1g}, A_{1g}, E_g, and B_{1g} Raman active modes of anatase TiO_2. The Raman spectrum of titania rods calcinated at 900 °C is presented in Figure 5b. Here, too, the spectrum containing bands at 144, 236,
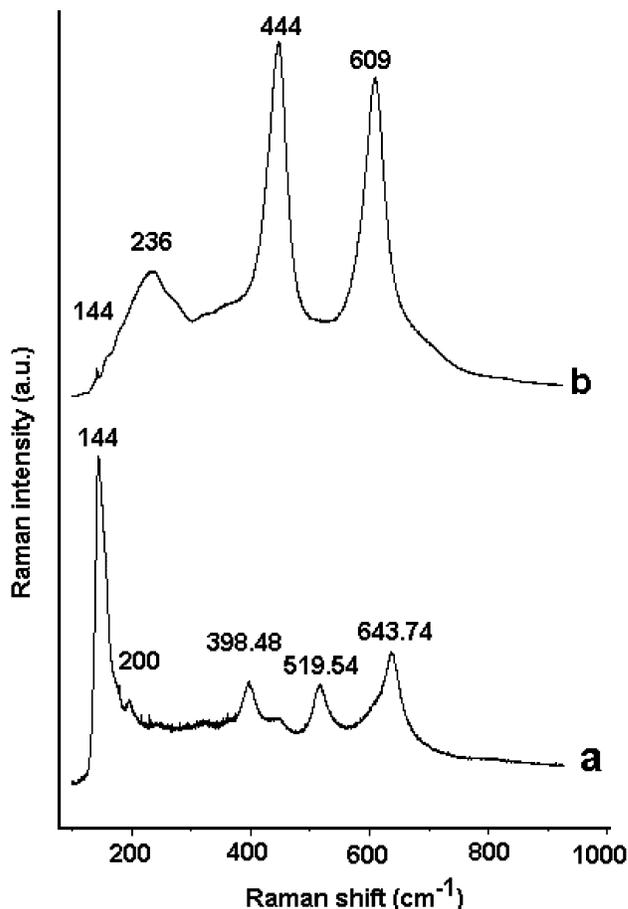
444, and 609 cm^{-1} matches previously reported spectra,[37] revealing the presence of pure rutile TiO_2.

The BET surface area measurement of as-prepared titanium glycolate was 6 m^2/g. After calcination of sample 2 to the anatase TiO_2 at 500 °C and to the rutile structure at 900 °C, the surface area increased to 50.5 m^2/g and 50.74 m^2/g, respectively.

A representative TEM image of the microwave-assisted, as-prepared titanium glycolate complex, is shown in Figure 6a, demonstrating that the morphology of the as-prepared products (sample 2) is rodlike. The size distribution is narrow, most of the rods having a width of 400 nm and a length of ∼6 μm. Upon heating, the shape of the as-prepared material did not change, implying that the rods are neither damaged nor formed during the 500 °C or 900 °C annealing process. The TEM image presented in Figure 6b confirms the roughness observed by SEM at the surface of the TiO_2 rods after annealing (Figure 2e). Furthermore, the HR-TEM image shown in Figure 6c reveals that the whole rod consists of ∼10-nm nanoparticles aggregated to a nanoporous geometry. The TiO_2 nanoparticles have a high degree of crystallinity, but they are not ordered to a particular orientation with respect to the rod axes. A typical example is highlighted in Figure 6c, showing a lattice spacing of 0.352 nm, which is equal to the *d* value of (101) planes for anatase. The insert in Figure 6c shows the corresponding electron diffraction patterns, features of polycrystalline anatase TiO_2 particles. The HR-TEM image of the rutile TiO_2 rod is shown in Figure 6d. In this case, the space between the lattice planes, 0.324 nm, fits the *d* value

(34) Willard, H. H.; Merritt, L. L.; Dean, J. A. *Instrumental Methods of Analysis*, 5th ed.; Van Nostrand: New York, 1974; p 502.
(35) Lei, Y.; Zhang, L. D.; Fan, J. C. *Chem. Phys. Lett.* **2001**, *338*, 231.
(36) Miao, L.; Tanemura, S.; Toh, S.; Kaneko, K.; Tanemura, M. *J. Cryst. Growth* **2004**, *264*, 246.

(37) Escobar-Alarcon, L.; Haro-Poniatowski, E.; Camacho-Lopez, M. A.; Fernandez-Guasti, M.; Jımenez-Jarquın, J.; Sanchez-Pineda, A. *Appl. Surf. Sci.* **1999**, *137*, 38.
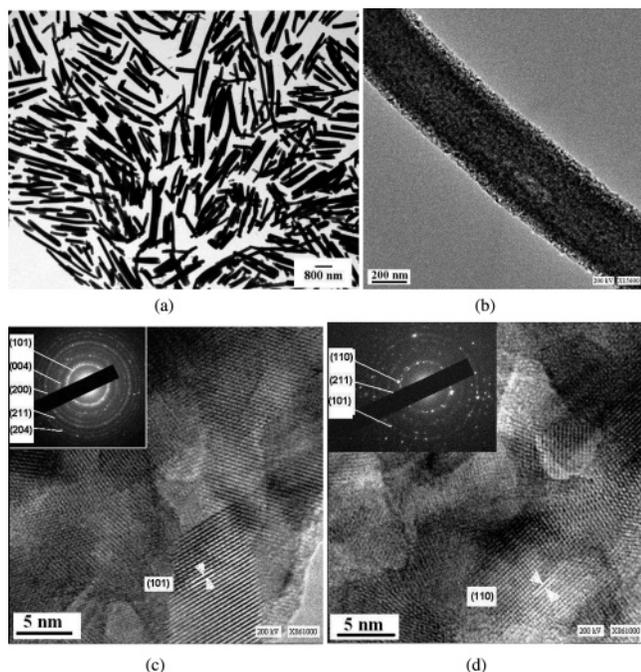
Figure 6. TEM images of (a) as-prepared titanium glycolate rods, (b) an individual anatase TiO_2 rod (after calcination), (c) HR-TEM image of an anatase TiO_2 rod demonstrating the obtained rods consisting of nanocrystallites with a polygonal shape and sized about 10 nm [insert shows the SAED pattern of polycrystalline anatase TiO_2 particles], and (d) HR-TEM image of a rutile TiO_2 rod [insert shows the SAED pattern of polycrystalline rutile TiO_2].

of the (110) planes for rutile. The insert demonstrates the corresponding electron diffraction patterns characteristic of polycrystalline rutile TiO_2 particles.

In the following section, we propose a mechanism for the formation of the submicrometer TiO_2 rods under solvothermal conditions using microwave irradiation. It is based on the reported mechanism for similar synthesis by a conventional heating method and our control experiements. A previous study showed that the ethylene glycol-mediated synthesis of metal oxide nanowires[32] requires heating a solution of titanium(IV) alkoxide in ethylene glycol at 170 °C for 2 h. This study mentioned that ethylene glycol can be used to form chainlike complexes with metal cations, which could readily aggregate into 1D nanostructures within an anisotropic medium. In the present case, similar results are achieved within 1−3 min under microwave rather than in 2 h of conventional heating. Microwaves provide very short non-ionizing electromagnetic energy waves that travel at the speed of light. When microwave energy passes through the matter, molecules of the matter having dipole moments will rotate and try to align themselves with the electric field.[38] There are two basic differences between microwave and conventional heating. (i) In a microwave-heated reactor, the average temperature of the solvent can be significantly higher than the atmospheric boiling temperature. This is due to the fact that the microwave power is dissipated over the entire volume of the solvent, where nucleation points necessary for boiling are absent.[39] The boiling can only occur at the reactor walls or at the solvent−air interface.[40] This results in a reversed temperature profile with a steady average reflux temperature above the classical boiling point, known as
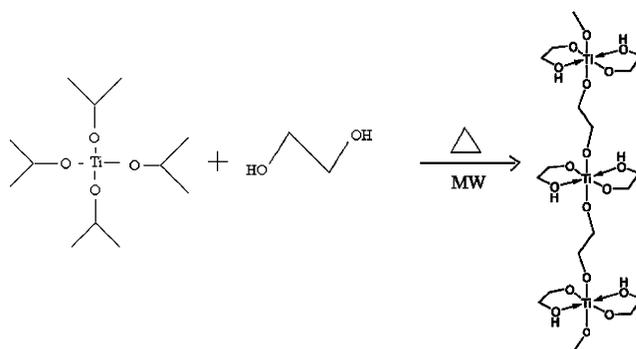
(38) Wang, W. Z.; Geng, Y.; Yan, P.; Liu, F. Y.; Xie, Y.; Qian, Y. T. *J. Am. Chem. Soc.* **1999**, *121*, 4602.

(39) Oman, D. M.; Dugan, K. M.; Killian, J. L.; Ceekala, V.; Ferekides, C. S.; Morel, D. L. *Sol. Energy Mater. Sol. Cells* **1999**, *58*, 361.

(40) Baghurst, D. R.; Mingos, D. M. P. *J. Chem. Soc., Chem. Commun.* **1992**, *9*, 674.

Figure 7. Reaction pathway for the fabrication of TiO_2 rods.

superboiling or superheating. These phenomena cause chemical reactions to proceed more quickly than in conventional heating.[25] (ii) The other difference between conventional and microwave heating relates to the temperature gradient in the sample.[41] In conventional heating, the outer surface of the sample is at a higher temperature than its interior, and heat flows from the surface inward. During microwave heating, because of the volumetric effect and the surface contact with air, the outer surface of the sample is colder than the interior. This creates a heat flow from the interior to the surface, i.e., an opposite direction relative to that for conventional heating.[42] If the bulk solvent and reactants absorb microwaves equally, then energy transfer and heating will occur to the allowed depth of penetration into the bulk mixture. Homogeneous reaction conditions can be established with thorough mixing,[41] and at equilibrium (chemical and thermal), the temperature of the reactants will be the same as that of the bulk solvent. Additionally, microwave dielectric heating does not occur at a molecule level; it is a semi-classical rather than quantum phenomenon and therefore depends on aggregates of molecules.[42] The differences between conventional and microwave heating arise because of the remote and volumetric nature of the microwave heating.[40]

As the immediate product of the microwave-based synthesis were nanorods of metal glycolate, we propose a model following the mechanism suggested for conventional heating.[32] The synthesis starts with the formation of the polymeric chains shown in Figure 7, which later act as the building blocks of the nanorods. Apparently, during the superheating treatment, the chainlike complexes elongate and consequently tend to aggregate into bundles. These bundles form the anisotropic rod shapes because of the stronger interaction between Ti and O atoms, compared to the van der Waals interactions between the two conjugated chains.

To gain control over the dimensions of the TiO_2 nanorods, additional experiments were carried out. The experimental conditions are summarized in Table 1. At first, the influence of the TiO_2 precursor concentration was examined. While preparing samples 2, 3, and 4, the amounts of tetra-isopropyl orthotitanate were 1, 2, and 0.2 mL, respectively. It was expected that the growth of the rods would be affected by the tetra-isopropyl orthotitanate concentration. In practice, the increase in the tetra-isopropyl orthotitanate concentration from 1 to 2 mL doubled the dimension of the formed titanium glycolate product, 800 nm in diameter and a length up to 20 μm (sample 3, Figure 8a). However, a decrease in the concentration from 1 to 0.2 mL did not affect the size and shape of the titanium glycolate product

(41) Meredith, R. J. *Engineers Handbook of Industrial Microwave Heating*; IEE: London, 1998.

(42) Kingston, H. M.; Jassie, L. B. *Introduction to Microwave Sample Preparation: Theory and Practice*; American Chemical Society; Washington, DC, 1988.
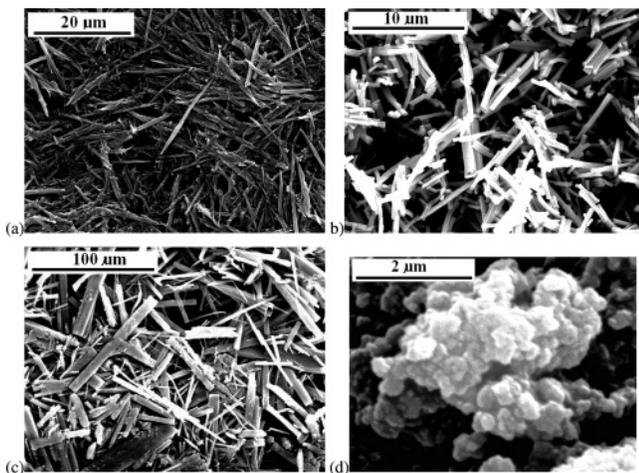
Figure 8. Scanning electron microscopy images of (a) sample 3, (b) sample 4, (c) sample 5, and (d) sample 6.

(Figure 8b). These experiments suggest that the stability of the nanorods is achieved only once they reach a given size. In other words, despite the low concentration of tetra-isopropyl orthotitanate, the rods grow to a stable size, and once this stability is achieved, larger rods can be formed, depending on the concentration. These results support the distinctiveness of microwaves over commercial heating. In microwave-based synthesis we do not regulate the temperature of the reaction, which is determined by the absorption of the molecules, the boiling point, and microwave intensity and duration. Below, we interpret the results in terms of the effective reaction temperature which, under constant irradiation intensity and duration, seems to be sensitive to the boiling point of the reactants.

In the second experiment, we examined the effect of the boiling point of the precursor by replacing tetra-isopropyl orthotitanate with titanium (IV) 2-ethylhexoxide ($C_{32}H_{68}O_4Ti$, boiling point 249 °C, Strem Chemical Co.) maintaining similar microwave conditions. After 3 min of microwave irradiation the synthesis yielded a white flocculate of a titanium glycolate complex. However, the dimensions were much larger than those in reference sample 2. The increase in the size of the rods, a result of the higher boiling point of the precursor, seems to be related to higher reaction temperatures. As mentioned above, in microwave irradiation the temperature is not necessarily uniform, depending on microwave absorption by the individual molecules. We suggest that the higher boiling point of titanium (IV) 2-ethylhexoxide

allowed a higher reaction temperature, resulting in faster kinetics and larger products.

Instead of ethylene glycol, a solvent with a higher boiling point (triethyleneglycol, 285 °C) was used for one of the trial experiments. The 3-min microwave reaction leads to the formation of TiO_2 particles with a diameter of 200 nm, rather than rods (sample 6, Figure 8d). However, in conventional heating, after using triethyleneglycol, Jiang et al. achieved titania wires.[17] It seems that the solvent's high boiling point resulted in a very high temperature of the reaction, with fast kinetics, leaving insufficient time for complexation. In other words, when using microwave, the high-boiling point solvent reached high temperatures within a short period and formed particles, but did not allow the formation of rods.

The formation of thinner TiO_2 rods was anticipated via the dilution of the solvent (EG) by the addition of isopropanol, due to small nucleation and growth. However, this approach resulted in the formation of nanosized titania particles. This might be understood by the addition of OH groups from the isopropanol, which facilitates the rate of hydrolysis. It further supports the fact that only an adequate amount of ethylene glycol plays an important role in the formation of titanium glycolate rods, and not the other solvents. In addition, the close boiling points of the solvent (ethylene glycol 198 °C) and the solute (232 °C) might enhance the coordination tendency of the solute and the solvent, thus influencing the superheating phenomena.

In conclusion, a simple and fast microwave irradiation-based method for the large-scale synthesis of submicrometer-sized TiO_2 rods with high surface area is demonstrated. The synthesis is carried out at normal atmospheric pressure, near the boiling temperature of the solvent. The reaction involves 1−3 min of microwave irradiation for the formation of a titanium glycolate complex, followed by 2 h of calcination under air to form anatase (500 °C) or rutile (900 °C) titania rods that consist of ∼10-nm-sized crystals in a nanoporous geometry. The effects associated with the precursor concentration, precursor structure, and the reaction solvents support the proposed mechanism. The latter involves microwave superheating phenomena that accelerate the formation of 1D submicrometer structures of a titanium glycolate complex.